

CASE REPORT

Open Access



Mutational analysis and protein expression of PI3K/AKT pathway in four mucinous cystadenocarcinoma of the breast

Yan Zheng^{1†}, Huaxiao Tang^{2†}, Qian Liu¹, Yujie Zhang¹, Peng Zhao³, Shukun Zhang^{1*} and Chengqin Wang^{3*}

Abstract

Introduction Primary mucinous cystadenocarcinoma of the breast (BMCA) is a rare neoplasm with few reports in the literature. Its molecular characteristics, prognosis, and treatment protocols are not well understood, and there is a lack of consensus concerning the optimal management of this condition.

Methods Four cases of clinical and pathological data were collected from 2018 to 2024. Next generation sequencing with a 654 cancer-associated gene panel was utilized to detect gene mutations. Immunohistochemistry was carried out to evaluate protein expression levels.

Results Firstly, we combined clinical imaging examinations and IHC to exclude the possibility of metastasis from ovarian or pancreatic origins. BMCA was composed of cystically dilated ducts lined by tall columnar mucin-containing epithelium. The morphological spectrum of MCA varied from MCA alone to MCA combined with carcinoma in situ (CIS) to MCA associated with invasive ductal carcinoma (IDC). *ER/PR/HER2* and *CK20* were all negative, while *CK7* and *GATA3* were positive by IHC in four cases. Although the prognosis of the other three patients was favorable during the follow-up periods of 13, 10, and 3 months, respectively, case 2# experienced a recurrence of the primary focus after 42 months. No lymphatic metastasis was identified in cases 1–4#. In addition, next-generation sequencing (NGS) identified 17 mutated genes and 25 mutation sites in four cases. *TP53*, *PIK3CA*, *AKT*, *PTEN*, and *RB1* were the highest frequency mutated genes. Given that *AKT* mutations typically refer to *AKT1* (E17K) rather than *AKT2* or *AKT3*, *AKT* protein expression was detected only in Case 2# (*AKT1*, E17K). *PTEN* protein was expressed in case 4# (corresponded to missense mutation), loss of *PTEN* expression were corresponding with splicing mutation in case 1#. In brief, *AKT* and *PTEN* protein expression could be corresponded to gene mutation in a certain extent. However, *PIK3CA* protein expression was positive in Case 2# but negative in Case 1#, which did not fully accordance with the NGS-detected missense mutations. No associated germline variations were detected. Additionally, neither *PDL-1* expression nor microsatellite instability-high (MSI-H) status was identified.

[†]Yan Zheng and Huaxiao Tang are co-first authors.

*Correspondence:
Shukun Zhang
zhangshukun0475@126.com
Chengqin Wang
wcq0879@126.com

Full list of author information is available at the end of the article



© The Author(s) 2025. **Open Access** This article is licensed under a Creative Commons Attribution-NonCommercial-NoDerivatives 4.0 International License, which permits any non-commercial use, sharing, distribution and reproduction in any medium or format, as long as you give appropriate credit to the original author(s) and the source, provide a link to the Creative Commons licence, and indicate if you modified the licensed material. You do not have permission under this licence to share adapted material derived from this article or parts of it. The images or other third party material in this article are included in the article's Creative Commons licence, unless indicated otherwise in a credit line to the material. If material is not included in the article's Creative Commons licence and your intended use is not permitted by statutory regulation or exceeds the permitted use, you will need to obtain permission directly from the copyright holder. To view a copy of this licence, visit <http://creativecommons.org/licenses/by-nc-nd/4.0/>.

Conclusion The tumorigenesis and development of BMCA may be regulated to the *PI3K/AKT* pathway. Consequently, a comprehensive genetic analysis of more cases could elucidate the molecular mechanisms underlying this rare tumor.

Keywords Mucinous cystadenocarcinoma, Breast cancer, *PI3K/AKT* pathway, *PIK3CA*, *AKT*, *PTEN*

Introduction

Intracellular mucin-producing carcinoma represents an extremely rare form of breast malignancy. According to the WHO classification, breast mucin-producing carcinomas are categorized into four distinct histologic subtypes: mucinous carcinoma, mucinous cystadenocarcinoma, columnar cell mucinous carcinoma, and signet ring cell carcinoma [1]. In 1984, Rosen reported a distinct multicystic form of ductal carcinoma of the breast, characterized by both gross and microscopic features, which was termed cystic hypersecretory ductal carcinoma [2]. In 1998, Koenig and Tavassoli summarized and reported four cases of breast tumors characterized by cystic lesions covered by mild columnar mucous cells, which were designated as primary mammary mucinous cystadenocarcinoma (MCA) [3]. In 2003, WHO classified it as a separate subtype of muco-secreting carcinoma. However, the name was removed from the 2012 edition of WHO without any further mention, and the 2019 edition of WHO re-incorporated the concept [4]. Up to now, less than 50 cases of MCA have been reported and most of them are case report. This rarity and its underlying molecular alterations had created difficulties in understanding BMCA tumorigenesis. Next-generation sequencing (NGS), characterized by high throughput, deep sequencing capacity, and exceptional sensitivity, has become a widely adopted tool in cancer research [5]. In this study, NGS technology was employed to conduct genomic profiling in four MCA patients, aiming to elucidate the gene mutations associated with MCA and investigate the molecular mechanisms underlying its onset and progression.

Materials and methods

Clinical materials

Four cases of primary mucinous cystadenocarcinoma of the breast, diagnosed from 2018 to 2024, were retrospectively reviewed by the Affiliated Hospital of Qingdao University and the Department of Pathology of Weihai Maternal and Child Health Hospital. Clinical and pathological data were collected, including age, location, tumor size, stage, ultrasound, morphological feature, immunophenotyping (*ER/PR/HER2*, *CK7/CK20*, *Ki67*, *P63*), lymphatic metastasis, follow-up time, prognosis, and treatment method.

Immunohistochemistry (IHC) analysis

All specimens were fully collected, fixed with 10% neutral formalin, dehydrated, embedded, and sliced 4 μ m thick. Paraffin sections were removed for dewaxing and hydration treatment, and the sections were placed in sodium citrate solution for antigen repair. After the sections were removed, they were naturally cooled and rinsed with PBS, incubated at 37°C for 1 h with primary antibody, rinsed again for 30 min with secondary antibody, rinsed with DAB for color development, hematoxylin staining, neutral gum sealing and microscopic examination. Anti-*P53* (dilution at 1:300), anti-*RBI* (dilution at 1:300), anti-*PTEN* (dilution at 1:300), anti-*PIK3CA* (dilution at 1:100), anti-*AKT* (dilution at 1:200), and sheep anti-rabbit (dilution at 1:100).

Next-generation sequencing (NGS) analysis

FFPE nucleic acid extraction kit was used to extract DNA from paraffin-embedded samples. Assay Kit Oubitds-DNA HS and Oubit 4.0 fluorometric quantifier were used to measure concentration. A library was constructed using a combination assay kit for detecting tumor polygene mutation. The amplified library was obtained after DNA interruption, terminal repair, splicing and PCR amplification. The amplified library and probe were hybridized in liquid phase, captured and enriched by magnetic bead method, PCR amplification to obtain the captured library, and the library quality control was performed. The sequencing was performed using Illumina MiseqDx sequencers, and the data were analyzed for bioinformatics. Mutation abundance $\geq 1\%$ is positive, and $< 1\%$ requires validation by other methodologies.

Result

Case report

Case1# It has been well documented in the previous literature [6].

Case2# A 40-year-old premenopausal female, with no significant past medical history, presented with a mass and watery nipple discharge in the left breast. Ultrasound examination revealed a 15 × 15 × 12 mm hypoechoic nodule at the 10 o'clock position in the left breast, located 2.5 cm away from the nipple. Magnetic resonance imaging (MRI) and mammography representations are displayed in Fig. 1A-C. Intraoperative frozen section analysis confirmed invasive breast cancer. Following eight cycles of chemotherapy (EC-T regimen), left breast expander

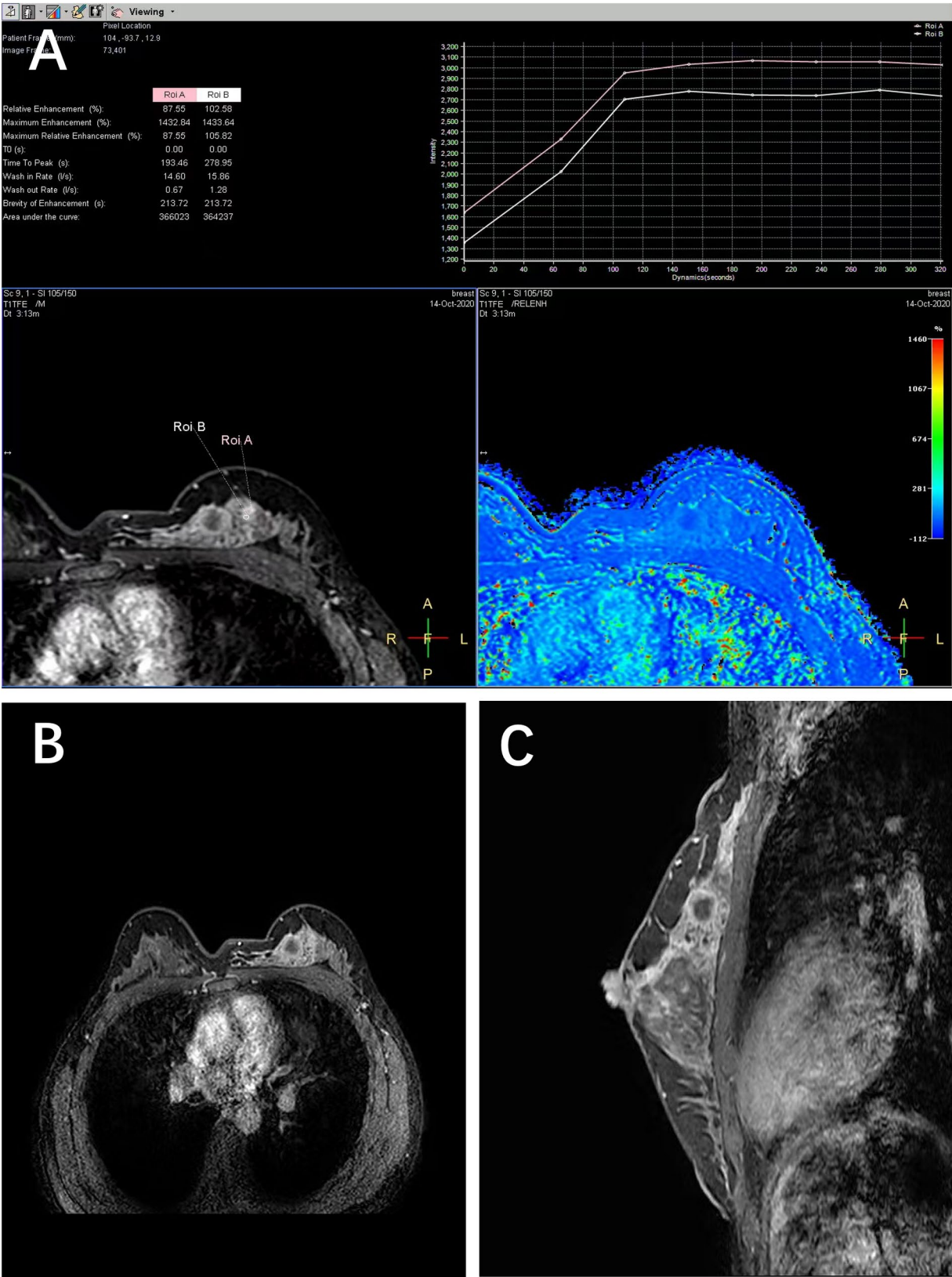


Fig. 1 (A-B) Ultrasonography demonstrated a hypoechoic mass with multiple hypoechoic nodules around it. (C) The mammography showed a high-density shadow in the upper quadrant of the right breast and the edge was rough

removal and prosthesis implantation were performed. However, a 15 × 10 mm tumor was identified at the original surgical site during follow-up at 42 months. The mass was resected under general anesthesia. Adjuvant radiotherapy was administered postoperatively. Currently the patient was healthy and alive after 6 months follow-up.

Case3# An outpatient examination of a 58-year-old postmenopausal woman revealed a hard and borderless mass in her left breast. Ultrasound showed BI-RAD was category 5. Mucinous cystadenocarcinoma was diagnosed by intraoperative freezing. Subsequently, left mastectomy and sentinel lymph node biopsy was performed. Gross examination of the specimen showed an indistinct boundary mass with gray, brittle and mucoid in some areas, measuring 20 × 12 × 10 mm. 5 cycles of chemotherapy with TCb regimen were given after surgery. After 10 months of follow-up, the patient was healthy and alive.

Case4# A 61-year-old postmenopausal woman was identified to have a mass measuring 6 × 3 × 1.8 mm in size with indistinct borders in the right breast; ultrasound examination classified the lesion as BI-RADS category 5. Extended and simple excision of the right breast and biopsy of the right anterior sentinel lymph node were performed. Adjuvant treatment did not give after the operation. She has been followed up for 3 months and preparing for subsequent radiotherapy and chemotherapy.

Furthermore, we integrated clinical imaging examinations with immunohistochemistry to rule out the possibility of metastasis from ovarian and pancreatic counterparts. The detailed clinicopathological features of the 4 cases in BMCA were showed in Table 1.

Histopathological features

In cases 1#, 3# and 4#, histopathology revealed lesions were composed of dilated cystic ducts lined by tall columnar mucin-containing epithelium, which represented cell stratification, tufting, micropapillary, and papillary architecture (Fig. 2A, C, and D). The nuclei were located at the base of neoplastic cells, round to oval, grade 1 to grade 2. Mucin also observed in the cystic cavity. Mild to moderate degrees of cytological atypia could be observed.

In case 2#, the primary tumor had an expansive pattern of growth with two adjacent regions (Fig. 2B). Microscopically, about 60% of the area was non-specific invasive carcinoma surrounded by a small cystic structure, which was coated with a complex growth of mucinous cells. Another portion of the tumor presents as mucinous cystadenocarcinoma in situ with stratification, tufting, micropapillary and papillary epithelial cells. A few embedded structures were also observed. The pathological features of the recurrent foci were similar to those in the other three cases.

Immunohistochemistry of four cases demonstrated that the tumor cells were positive for CK7, GATA3, while negative for CK20, ER/PR/HER2. The majority of the

Table 1 Clinicopathological data in 4 cases of primary mucinous cystadenocarcinoma of the breast

	Case1#	Case2#	Case3#	Case4#
Admission date	2018	2020	2023	2024
Age, years	66	40	58	61
Location	Right	Left	Left	Right
Tumor size, cm	2.5 × 2.5 × 2.0	1.9 × 1.8 × 1.7	2.0 × 1.2 × 1.0	6.0 × 3.0 × 1.8
Stage	PT2N0	PT1cN0	PT2N0	PT2N0
Ultrasound	BI-RAD 5	BI-RADS 4B	BI-RAD 5	BI-RAD 5
IDC/DCIS	DCIS	IDC + DCIS	DCIS	DCIS
ER/PR/HER2	-/-/-	-/-/-	-/-/-	-/-/-
CK7/CK20	+/-	+/-	+/-	+/-
Ki-67	60%	50%	15%	20%
Lymphatic Metastasis	No	No	No	No
Follow-up, months	13	48	10	3
Prognosis	Well	Relapse	Well	Well
Treatment method	Radical mastectomy	Excision of breast mass + excision of left breast subcutaneous gland + sentinel lymph node biopsy + dilator implantation	Simple left mastectomy + sentinel lymph node biopsy; 5 cycles of chemotherapy with TCb regimen were given after surgery	Excision of breast mass + excision of right breast subcutaneous gland + sentinel lymph node biopsy + dilator implantation

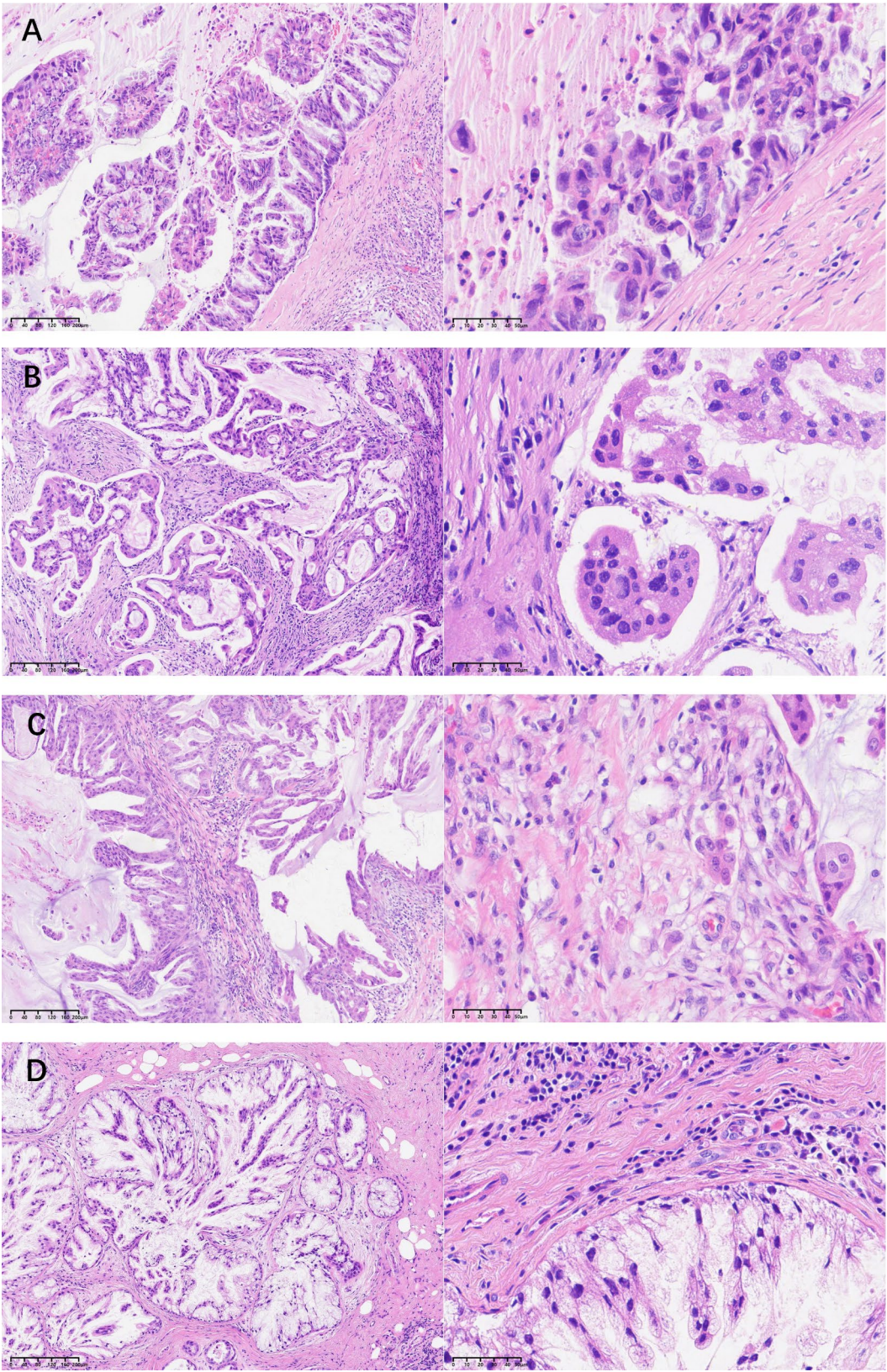


Fig. 2 (A) Low and higher power demonstrates a BMCA lesion in case 1–4 # (H&E, low is 100X, higher is 400X)

P63 was negative in the lateral myoepithelial cells, while only a small proportion showing positivity. The Ki-67 index ranged from 15 to 60%, and it was notably higher in regions exhibiting mild morphological cellular atypia.

Molecular features

A total of 654 genes were sequenced utilizing NGS. The information regarding the mutated genes is summarized in Table 2.

In four cases, 17 mutated genes and 25 mutated sites were identified. Additionally, *TP53*(16%,4/25), *PIK3CA*(12%,3/25), *AKT*(8%,2/25), *PTEN*(8%,2/25), and *RBI*(8%,2/25) were the highest frequency mutated genes according to the NGS results of the 4 cases. Five types of mutations were observed: missense mutation, frame-shift mutation, splicing mutation, nonsense mutation and copy number amplification. Interestingly, *TP53* was mutated as missense mutation, splicing, and nonsense mutation. *TP53* mutation was detected in all four cases. *TP53* Q331* (Allele frequency=57.65%) and *AKT1* E17K (Allele frequency=53.78%) exhibited the highest mutation rates in our dataset. *PIK3CA* mutations was detected in both case 1# and 2#, *AKT* mutation was present in case 2# and 3#, and *PTEN* mutations were observed in case 1# and case 4#. Emphatically, E545K, H1047L, and N345K were the common hot-spot mutations in *PIK3CA*,

which were located in the *PIK* helical, *PI3K/PI4K*, and C2 *PI3K* domain, respectively (Fig. 3A). The E17K variant, characterized by a nucleotide substitution at position 49 in exon 4, was the most commonly observed *AKT1* variant and is highly prevalent in breast cancer (Fig. 3B). In addition, the *PTEN* gene experienced a frameshift starting from the codon encoding threonine 319, potentially introducing a termination codon within the new reading frame and resulting in mRNA degradation. Splicing of the *PTEN* gene led to the loss of protein expression (Fig. 3C).

No associated variations were identified in germline analysis. The tumor mutation burden (TMB) was 10.8Muts/Mb, 3.93Muts/Mb, 2.95Muts/Mb, 5.89Muts/Mb in case1-4, respectively. Neither *PD-L1* expression nor microsatellite instability high (MSI-H) was detected in any of the cases examined.

Protein expression

To validate the consistency between NGS mutation results and the protein expression of *TP53*, *RBI1*, *PTEN*, *PIK3CA*, *AKT*, immunohistochemistry was performed. Abnormal expression of *TP53* protein in invasive tumor cells were defined as an overexpression pattern (OE, strong and diffuse nuclear staining in at least 80% of tumor cells), null-type pattern (NT, complete absence of

Table 2 Summary of the mutations identified in 4 cases of primary mucinous cystadenocarcinoma of the breast

Case	Gene	Exon	DNA sequence change	Amino acid change	Allele frequency	Type of mutation
Case1#	PIK3CA	10	c.1633G>A	p.E545K	1.95%	Missense mutation
		21	c.3140 A>T	p.H1047L	15.89%	Missense mutation
	PTEN	8	c.802-2 A>T	--	12.04%	Splicing mutation
	TP53	8	c.818G>T	p.R273L	18.18%	Missense mutation
	NF1	5	c.574 C>T	p.R192	5.17%	Missense mutation
	RB1	9	c.869dup	p.N290Kfs	23.01%	Frameshift mutation
	CBL	8	c.1227 + 1G>A	--	6.0%	Splicing mutation
	NAV3	33	c.6025G>A	p.D2009N	6.48%	Missense mutation
	NBN	11	c.1445G>A	p.R482K	6.32%	Missense mutation
	RAD51	4	c.246dup	p.R83Qfs	3.14%	Frameshift mutation
Case2#	SDHD	4	c.392_393delinsCC	p.F131S	5.67%	Missense mutation
		5	c.1035T>A	p.N345K	7.9%	Missense mutation
		7	c.743G>A	p.R248Q	8.99%	Missense mutation
		10	c.829 C>G	p.L277V	7.14%	Missense mutation
Case3#	AKT1	3	c.49G>A	p.E17K	53.78%	Missense mutation
		6	c.635_653del	p.F212Cfs	13.92%	Frameshift mutation
		15	c.2098 A>G	p.K700E	12.46%	Missense mutation
		-	Copy number amplification	CN=8.09	--	
		2	c.49T>A	p.S17T	14.17%	Missense mutation
Case4#	GATA3	5	c.925-3_925-2del	--	12.89%	Splicing mutation
		8	c.956_986del	p.T319lfs	19.0%	Frameshift mutation
	TP53	9	c.991 C>T	p.Q331*	57.65%	Nonsense mutation
	GABRA6	4	c.345 C>A	p.D115E	14.59%	Missense mutation
	PTPN2	2	c.118 C>A	p.P40T	6.45%	Missense mutation
	RB1	22	c.2325 + 2_2325 + 26del	--	25.95%	Splicing mutation

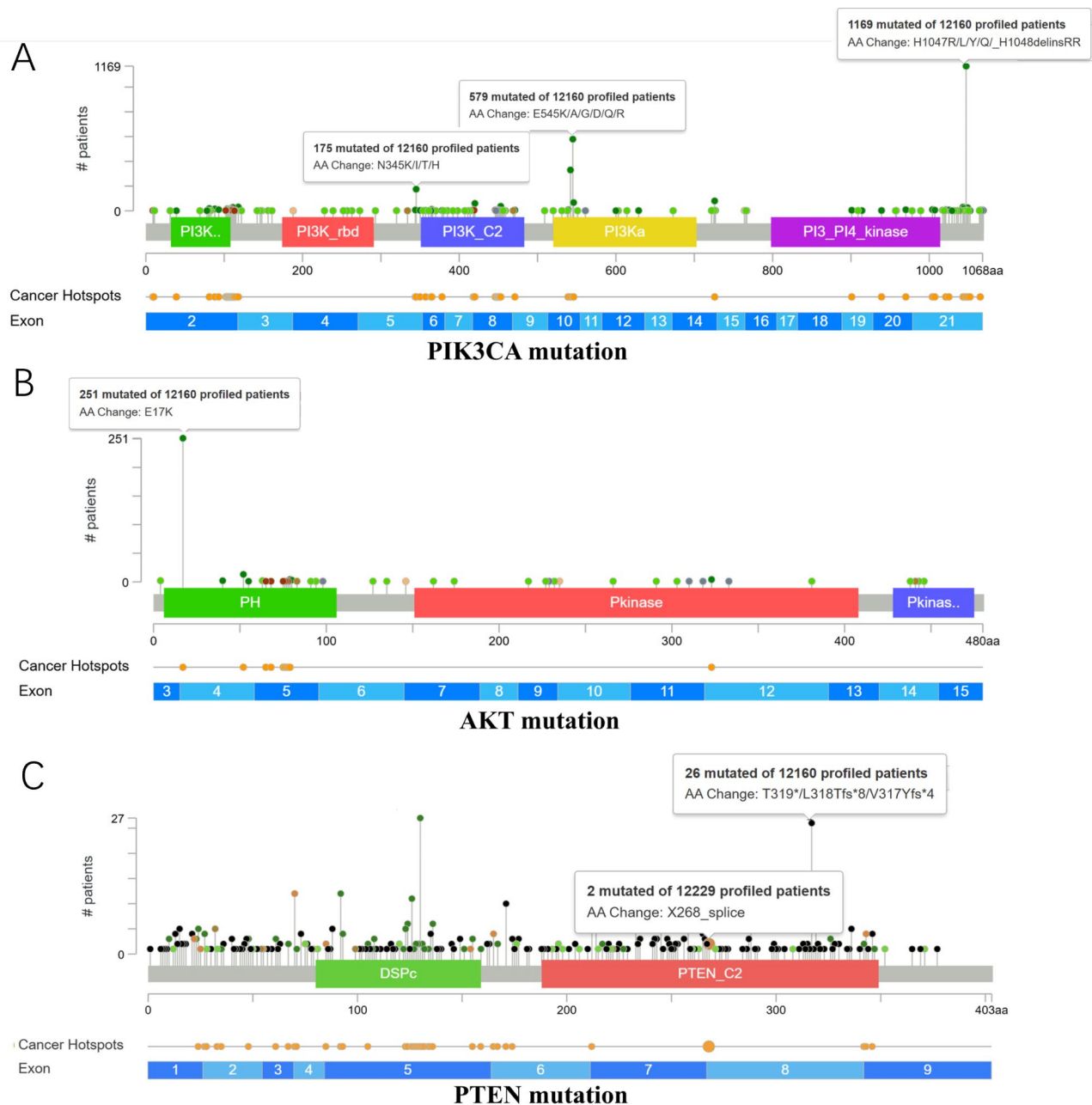


Fig. 3 Schematic diagram of *PIK3CA*, *AKT*, *PTEN* mutation sites from cBioPortal data

expression, with a variable intensity of staining in stromal cells acting as an internal control [7]. We identified that *TP53* was overexpressed through immunohistochemistry in four patients, corresponding to missense mutation, frameshift mutation, and nonsense mutation (Fig. 4A). For the *RB1* gene, a complete loss of *RB1* protein nuclear expression was observed, corresponding to the splicing mutation in case 4# (Fig. 4B). In contrast, *RB1* nuclear expression remained positive and was associated with the frameshift duplication in case 1# (Fig. 4C). Furthermore, the *PI3K/AKT* pathway can be activated through *PIK3CA* mutations, *AKT1* mutations or *PTEN* loss in

breast cancer [8]. *PIK3CA* protein was positive in case2# (Fig. 4D), but negative in case1# (Fig. 4E), which did not entirely align with NGS missense mutation in a certain extent. Because *AKT* mutations generally refer to *AKT1*(E17K) rather than *AKT2* or *AKT3*. *AKT* expression was undetectable in case2# (Fig. 4G), and was exclusively expressed in case3# (Fig. 4F). *PTEN* protein was detected in case4# (Fig. 4I), while the loss of *PTEN* protein expression corresponded to a splicing mutation in case1# (Fig. 4H).

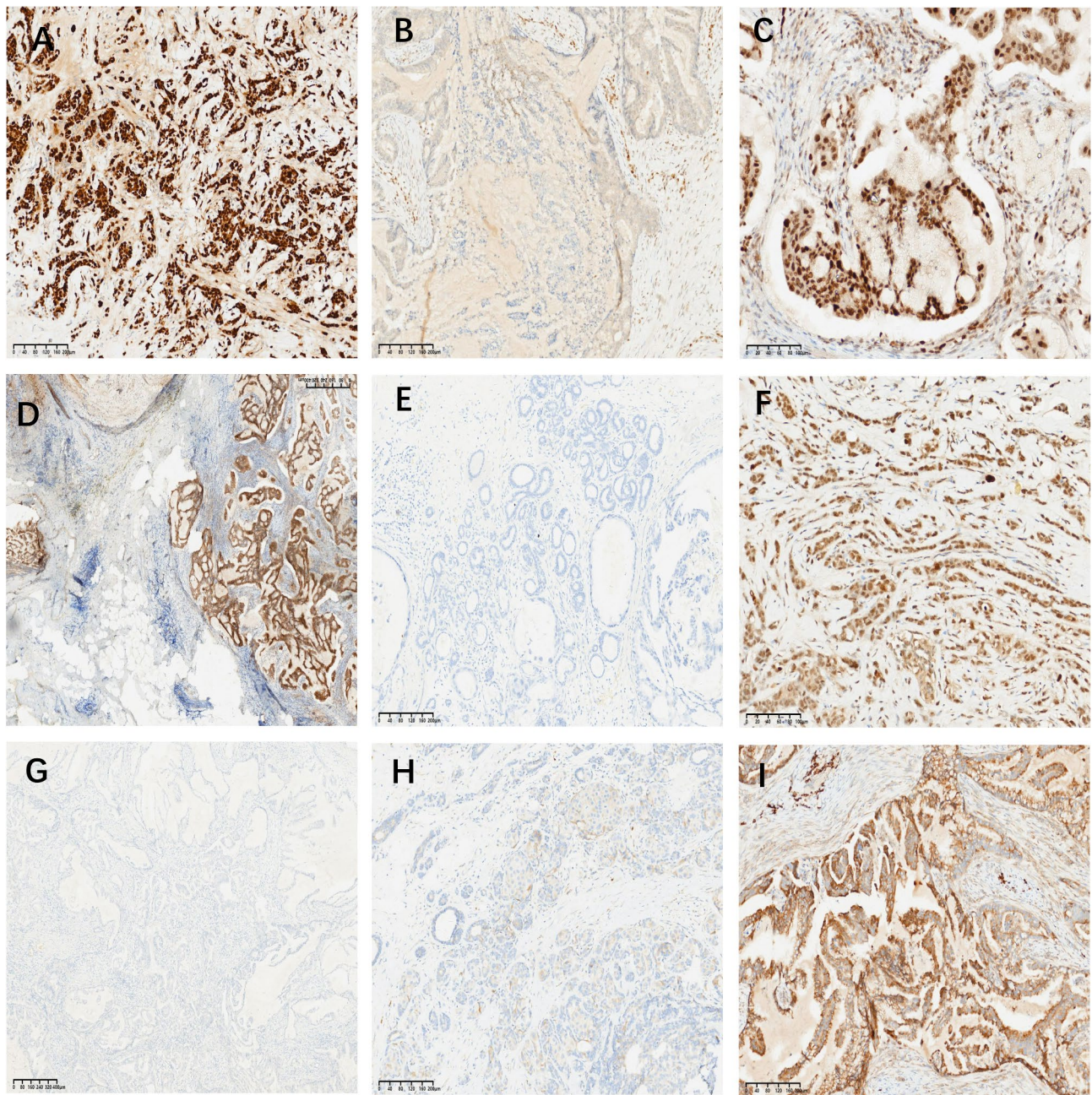


Fig. 4 (A) *P53* is overexpression in case 1–4# (IHC, dilution at 1:300, 100X). (B) *RB1* is negative in case 4# (IHC, dilution at 1:300, 100X). (C) *RB1* is positive in case 1# (IHC, dilution at 1:300, 100X). (D) *PIK3CA* is positive in case 2# (IHC, dilution at 1:100, 100X). (E) *PIK3CA* is negative in case 1# (IHC, dilution at 1:100, 100X). (F) *AKT* is positive in case 3# (IHC, dilution at 1:200, 100X). (G) *AKT* is negative in case 2# (IHC, dilution at 1:200, 100X). (H) *PTEN* protein is loss in case 1# (IHC, dilution at 1:300, 100X). (I) *PTEN* protein is expressed in case 4# (IHC, dilution at 1:300, 100X)

Discussion

Primary mucinous cystadenocarcinoma of the breast is a rare neoplasm that exhibits marked morphological resemblance to mucinous cystadenocarcinomas of the ovary or pancreas [9]. Currently, we have systematically reviewed 41 publications from the Pubmed database, and the clinicopathological features of these cases, including our own, have been consolidated in Table 3, thereby

contributing to the existing knowledge base on breast mucinous cystadenocarcinoma.

In general, MCA typically manifests as a well-defined solid or cystic mass [10]. Histomorphologically, the cyst wall is lined by mucus-rich tumor cells exhibiting multilayering, clustering, and papillary hyperplasia, with nuclei positioned basally [11]. Our cases demonstrated abundant intracellular mucin alongside extracellular mucin within the centers of cystically dilated ducts. The

Table 3 Summary of the clinicopathologic features of 44 cases (include our cases)

Age, years	
Range, years	40–96
Average, years	58.61
Tumor size, mm	
Range, mm	8–180
Average, mm	46.79
Location	
Left	22/44(50.00%)
Right	15/44(34.09%)
Left + Right	1/44(2.27%)
NA.	6/44(13.64%)
ER/PR/HER2	
-/-/-	35/44(79.55%)
+/-/-	1/44(2.27%)
+ /+/-	3/44(6.82%)
-/-/+	5/44(11.36%)
Morphology	
MCA + DCIS	19/39(48.72%)
MCA in situ	8/38(21.05%)
Metastasis	
Distance metastasis	2/44(4.55%)
Lymph node metastasis	8/44(18.18%)
Follow up, months	
Range, months	3–108
Average, months	19.76
NA.	7
Prognosis	
Alive	34/44(77.27%)
DOD	3/44(6.82%)
NA.	7/44(15.91%)

morphological spectrum of MCA extends from MCA alone to MCA + CIS (carcinoma in situ) to MCA + IDC (invasive ductal carcinoma). MCA may be accompanied by common DCIS (with/without mucus). Pericapsular myoepithelial markers were mostly negative, and a few pericapsular myoepithelial markers were visible (Supplementary Fig. 1), the latter being the carcinoma in situ form of MCA, which is also evidence of breast primary. In contrast, mucinous carcinoma is characterized by a lake of mucus without a capsular wall structure, a diffuse distribution of extracellular mucus surrounding tumor cell masses, and is more common in breast cancer [12]. In terms of immunophenotypic features, MCA was mostly triple-negative, while mucinous carcinoma was mostly hormone receptor-positive.

Nayak had presented with local recurrence 8 years (96 months) after lumpectomy with negative margins [13]. Likewise, our Case 2# experienced a recurrence of the primary focus after 42 months, which highlighting MCA may have a long-term risk of local recurrence. Among 44 samples, 8 were associated with lymph node metastasis. The reported cases were followed up for 3 to 108 months,

and only 3 patients died from other diseases (excluding those lost to follow-up). The findings indicate that the prognosis of primary breast MCA is generally favorable; however, further long-term follow-up studies with larger cohorts are still required.

Immunohistochemically, among the established molecular phenotypes, the majority of the cases were triple-negative expression of *ER*, *PR*, and *HER2*, whereas a minority demonstrated *HER2* positivity. IHC testing of lineage markers is critical to accurately diagnose primary breast MCA. Unlike primary pancreatic and ovarian MCAs, which are typically *CK7* and *CK20* positive, breast MCA is usually *CK20* negative.

Advances in molecular techniques have broadened our understanding and perspectives on the pathobiology and behavior of breast cancer [14]. Determining the genetic profile of tumors may enhance classification, improve prognostic accuracy, and offer therapeutic targets for mucinous cystadenocarcinoma of the breast [11]. However, the majority of sporadic cases only described the histopathological features in BMCA. The histogenesis and biological behavior of this neoplasm remain uncertain. NGS studies have established at least 40 driver genes in breast cancers, and the most frequently mutated genes were *TP53*, *PIK3CA*, *GATA3*, *MYC*, *CCND1*, *PTEN*, *FGFR1*, *RB1*, *ERBB2*, and *MAP3K1* [15]. Generally, mutations are infrequent in breast cancers, with only the three most common mutations (*TP53*, *PIK3CA*, and *GATA3*) occurring at frequencies exceeding 10% [16]. In our study, *TP53*, *PIK3CA*, *GATA3*, *PTEN*, and *RB1* were also mutated, which were consistent with the findings reported by Nik-Zainal. To date, only 3 MCA cases have been sequenced in the literature [9, 11, 17], and their sequencing data have been reviewed and summarized in Table 4. Previous sequencing results showed that *TP53* and *PIK3CA* were most frequently mutated [9, 11, 17]. In our cases, *TP53* and *PIK3CA* were also mutated, thereby confirming the critical role of *TP53* and *PIK3CA* in the occurrence and progression of MCA.

Phosphatidylinositol 3-kinase (*PI3K*)/protein kinase B (*PKB*, also known as *AKT*) pathway mutations are commonly observed in breast cancer (20–40%) and represent significant factors contributing to aggressive tumor behavior and treatment resistance [18]. *PI3K*/*AKT* mutations are more frequent in hormone receptor-positive (HR+) breast cancer compared to other subtypes [19]. The *PI3K*/*AKT* inhibitors activity is still at early-phase development in metastatic TNBC [20]. Key mechanisms leading to pathway deregulation include *PIK3CA* mutations, *AKT* mutations or *PTEN* loss [21]. *PI3KCA* mutations lead to activation of α -*PI3K*, which enhances phosphorylation and accumulation of *PIP3* in cell membranes. *PTEN* is a phosphatase that dephosphorylates *PIP3* to *PIP2*, blocking *PIP3* as a key cellular second

Table 4 Review of the genetic profile in the literatures of primary mucinous cystadenocarcinoma of the breast

Case	Gene	Exon	DNA sequence change	Amino acid change	Allele frequency	Type of mutation
[9]	<i>PIK3CA</i>	9	C.1636 C > A	P.Q546K	25.67%	Missense mutation
[11]	<i>PIK3CA</i>	-	C.3140 A	p.H1047R	23.9%	Missense mutation
	<i>KRAS</i>	-	C.35G	p.G12V	55.5%	Missense mutation
	<i>MAP2K4</i>	-	C.257_258del	p. R86Tfs	30.5%	Frameshift deletion
	<i>RB1</i>	-	C.277 C	-	55.2%	Missense mutation
	<i>KDR</i>	-	C.521G	-	14.1%	Missense mutation
	<i>PKHD1</i>	-	C.6453G	-	30.9%	Missense mutation
	<i>TERT</i>	-	C.1006G	-	15.5%	Missense mutation
	<i>TP53</i>	-	C.476 C	-	44.0%	Missense mutation
	<i>BAP1</i>	5	C.362delG	P.G121fs	6.5%	Frameshift deletion
[17]	<i>RB1</i>	24	C.2518delG	P.G840fs	9.4%	Frameshift deletion
	<i>TP53</i>	4	C.G329C	PR110P	7.7%	Missense mutation

messenger to transmit extracellular signals, and then activating *AKT* to promote cell proliferation [22]. In our study, *PIK3CA* in case 1# and 2# exhibited mutations at E545K, H1047R, and N345K, all of which are known hotspot mutations. Additionally, Lin LH and Lei T also detected *PIK3CA* mutation with Q546K and H1047R [11, 17]. *PIK3CA* mutations are associated with poor outcomes and resistance to chemotherapy in *HR+ / Her2-* breast cancer patients [23]. However, *PIK3CA* protein was negative in case1# but positive in case2#, which was not well accordance with NGS missense mutation. It may indicate that IHC may lead to inaccurate results of *PIK3CA*, which was still based on NGS and PCR. It is also possible that protein degradation occurred due to the prolonged preservation time of the specimens. Nonetheless, the prognostic implications of *PIK3CA* mutations in MCA remain unclear, necessitating further investigation with additional data. To date, relevant studies have indicated that among the *AKT* family, *AKT1* is most closely associated with *PIK3CA* gene mutation [24]. Mutation of *AKT1* and *AKT3* were firstly detected in our study, whereas no mutations in any subtype of *AKT* were identified in other studies [9, 11, 17]. *PTEN* contains two key domains for its tumor suppression function: the phosphatase domain and the C2 domain [25]. For the first time, we detected *PTEN* frameshift deletion and splicing mutations located in the C2 tensin-type domain. In brief, *AKT* and *PTEN* protein expression correlated with gene mutations in our cases.

Currently, tubular, mucinous, and neuroendocrine tumors were classified into the luminal subtype, while mucinous cystadenocarcinoma, medullary, and metaplastic carcinomas were classified into the BLBC subtype [26]. BMCA was belong to a typical triple-negative breast cancer (TNBC) from the point of immunophenotype [9]. It is an interesting paradox that some special subtypes with a good prognosis, such as MCA and secretory carcinomas, are categorized within the BLBC group, which is generally associated with a poor outcome [27–28]. Due

to the rarity of BMCA, rare studies have yet investigated genetic alterations in this type of tumor. As a small case series, our findings are inherently limited by the lack of statistical power and generalizability. By contrast, other types of TNBCs, such as secretory carcinoma with recurrent *ETV6::NKRT3* rearrangement, have been extensively studied, identifying specific genetic alterations that could be targeted with therapy [29]. Therefore, further studies are needed to validate the relevance of *PI3K/AKT* pathway in larger cohorts of BMCA patients and to explore the potential role of *PIK3CA* alterations in this tumor.

In conclusion, this study presents the first report of four cases detailing the comprehensive genetic profiles and *PIK3CA/AKT/PTEN* protein expression in BMCA. The tumorigenesis and development of BMCA may be regulated to the *PI3K/AKT* pathway. At present, targeted therapy to the *PI3K/AKT* pathway in breast cancer is being to approved, which could bring a new therapeutic strategy for BMCA.

Acknowledgements

Supported by Natural Science Foundation of Shandong Province (ZR2022MH206) and the National Natural Science Foundation of China (81672606).

Author contributions

Y.Z. and H.T. performed the sample collection and research and wrote the paper; Q.L. and Y.J.Z. performed the immunohistochemistry analysis; P.Z. provided the clinical cases; C.W. and S.Z. contributed to the research design and revision of the manuscript and gave the final approval of the manuscript.

Funding

Supported by Natural Science Foundation of Shandong Province (ZR2022MH206) and the National Natural Science Foundation of China (81672606).

Data availability

No datasets were generated or analysed during the current study.

Declarations

Conflicts of interest

The authors have disclosed that they have no significant relationships with or financial interest in any commercial companies pertaining to this article.

Author details

¹Shandong Provincial Key Medical and Health Laboratory of Geriatric Gastrointestinal Tumor Pathology; Department of Pathology, Weihai Municipal Hospital, Cheeloo College of Medicine, Shandong University, Weihai, China

²Department of Pathology, the Affiliated Weihai Second Municipal Hospital of Qingdao University, Weihai, China

³Department of Pathology, the Affiliated Hospital of Qingdao University, Qingdao, Shandong 266000, China

Received: 6 February 2025 / Accepted: 14 April 2025

Published online: 28 May 2025

References

1. WHO. WHO Classification of Tumours Editorial Board. Breast Tumours. Vol 2. 5th Ed. Lyon, France: IARC. 2019.
2. Rosen PP, Scott M. Cystic hypersecretory duct carcinoma of the breast. *Am J Surg Pathol*. 1984;8(1):31–41.
3. Koenig C, Tavassoli FA. Mucinous cystadenocarcinoma of the breast. *Am J Surg Pathol*. 1998;22(6):698–703.
4. Tan PH, Ellis I, Allison K, et al. WHO classification of tumours editorial board. The 2019 world health organization classification of tumours of the breast. *Histopathology*. 2020;77(2):181–5.
5. Levy SE, Boone BE. Next-Generation sequencing strategies. *Cold Spring Harb Perspect Med*. 2019;9(7):a025791.
6. Wang X, Li Y, Zhao P, et al. Primary mucinous cystadenocarcinoma of the breast: a clinicopathologic analysis of one case and review of the literature. *Int J Clin Exp Pathol*. 2020;13(10):2562–8.
7. Anderson SA, Bartow BB, Harada S, et al. p53 protein expression patterns associated with TP53 mutations in breast carcinoma. *Breast Cancer Res Treat*. 2024;207(1):213–22.
8. Xing Y, Lin NU, Maurer MA, et al. Phase II trial of AKT inhibitor MK-2206 in patients with advanced breast cancer who have tumors with PIK3CA or AKT mutations, and/or PTEN loss/pten mutation. *Breast Cancer Res*. 2019;21(1):78.
9. Chen WY, Hu YH, Tsai YH, et al. Mucinous cystadenocarcinoma of the breast harbours TRPS1 expressions and PIK3CA alterations. *Histopathology*. 2024;84(3):550–5.
10. Gong Y, Geng X, Liu Y, et al. Mucinous cystadenocarcinoma of the breast with bone metastases: first case report and literature review. *Oncol Res Treat*. 2024;47(3):97–103.
11. Lin LH, Hernandez O, Zhu K, et al. Genetic profile of primary mucinous cystadenocarcinoma of the breast-A case report. *Breast J*. 2021;27(9):731–4.
12. Lu K, Wang X, Zhang W, et al. Clinicopathological and genomic features of breast mucinous carcinoma. *Breast*. 2020;53:130–7.
13. Nayak A, Bleiweiss JJ, Dumoff K, et al. Mucinous cystadenocarcinoma of the breast: report of 2 cases including one with Long-Term local recurrence. *Int J Surg Pathol*. 2018;26(8):749–57.
14. Garrido-Castro AC, Lin NU, Polyak K. Insights into molecular classifications of Triple-Negative breast cancer: improving patient selection for treatment. *Cancer Discov*. 2019;9(2):176–98.
15. Nik-Zainal S, Davies H, Staaf J, et al. Landscape of somatic mutations in 560 breast cancer whole-genome sequences. *Nature*. 2016;534(7605):47–54.
16. Cancer Genome Atlas Network. Comprehensive molecular portraits of human breast tumours. *Nature*. 2012;490(7418):61–70.
17. Lei T, Shi YQ, Chen TB. Mammary mucinous cystadenocarcinoma with long-term follow-up: molecular information and literature review. *Diagn Pathol*. 2023;18(1):13.
18. Cerma K, Piacentini F, Moschetti L, et al. Targeting PI3K/AKT/mTOR pathway in breast cancer: from biology to clinical challenges. *Biomedicine*. 2023;11(1):109.
19. Razavi P, Chang MT, Xu G, et al. The genomic landscape of Endocrine-Resistant advanced breast cancers. *Cancer Cell*. 2018;34(3):427–e4386.
20. Massihnia D, Galvano A, Fanale D, et al. Triple negative breast cancer: shedding light onto the role of pi3k/akt/mTOR pathway. *Oncotarget*. 2016;7(37):60712–22.
21. Engelman JA. Targeting PI3K signalling in cancer: opportunities, challenges and limitations. *Nat Rev Cancer*. 2009;9(8):550–62.
22. Glaviano A, Foo ASC, Lam HY, et al. PI3K/AKT/mTOR signaling transduction pathway and targeted therapies in cancer. *Mol Cancer*. 2023;22(1):138.
23. Mosele F, Stefanovska B, Lusque A, et al. Outcome and molecular landscape of patients with PIK3CA-mutated metastatic breast cancer. *Ann Oncol*. 2020;31(3):377–86.
24. Basu A, Lambring CB. Akt isoforms: A family affair in breast Cancer. *Cancers (Basel)*. 2021;13(14):3445.
25. Post KL, Belmadani M, Ganguly P, et al. Multi-model functionalization of disease-associated PTEN missense mutations identifies multiple molecular mechanisms underlying protein dysfunction. *Nat Commun*. 2020;11(1):2073.
26. Weigelt B, Horlings HM, Kreike B, et al. Refinement of breast cancer classification by molecular characterization of histological special types. *J Pathol*. 2008;216(2):141–50.
27. Tsang JYS, Tse GM. Molecular classification of breast Cancer. *Adv Anat Pathol*. 2020;27(1):27–35.
28. Botti G, Cantile M, Collina F, et al. Morphological and pathological features of basal-like breast cancer. *Transl Cancer Res*. 2019;8(Suppl 5):S503–9.
29. Cardoni A, De Vito R, Milano GM, et al. A pediatric case of High-Grade secretory carcinoma of the maxillary sinus with ETV6::NTRK3 gene fusion, therapeutic implications, and review of the literature. *Pediatr Dev Pathol*. 2023 Jan-Feb;26(1):59–64.

Publisher's note

Springer Nature remains neutral with regard to jurisdictional claims in published maps and institutional affiliations.